Journal of Applied Informatics and Computing (JAIC)
Vol.9, No.3, June 2025, pp. 1074~1081
e-ISSN: 2548-6861

Design and Implementation of a 3-Axis UAV Drone Gimbal Rig for Testing Stability and Performance Parameters in the Laboratory

Ryan Satria Wijaya [1]*, Zulpriadi [2]*, Senanjung Prayoga [3]*, Rifqi Amalya Fatekha [4]*
* Jurusan Teknik Elektro, Prodi Teknik Robotika, Politeknik Negeri Batam, Batam, Indonesia
ryan@polibatam.ac.id [1], zulpriadi11@gmail.com. [2], senanjung@polibatam.ac.id [3], rifki@polibatam.ac.id [4]

Article Info

Article history:

Received 2025-04-30
Revised 2025-06-10
Accepted 2025-06-17

Keyword:

3-Axis UAV Gimbal Rig, Real-Time Monitoring, UAV Dynamics Arduino Controller, Rotary Encoder LPD3806-600BM-G5g.

ABSTRACT

This study designs a 3-axis UAV gimbal rig for testing stability and performance before deployment in real-world flight conditions. The gimbal rig simulates the vertical, lateral, and longitudinal axes to ensure reliable operation in various scenarios. Made from lightweight aluminum alloy, the structure minimizes vibrations and maintains rigidity during testing. For precise motion tracking, each axis is equipped with an LPD3806- 600BM-G5 rotary encoder, offering accurate feedback on movement. The Arduino Nano processes the encoder data, displaying real-time results on a 16x2 LCD with an I2C interface for easy monitoring. Additionally, a push-button system enables users to switch between different readings for each axis. This setup aids researchers in analyzing UAV dynamics and refining both firmware and hardware. Future enhancements may include wireless data logging and integration of machine learning techniques to predict maintenance needs, further supporting UAV stability testing in various applications, including aerospace, defense, and commercial use.

I. INTRODUCTION

This Unmanned Aerial Vehicles (UAVs) have revolutionized numerous sectors, ranging from military applications to commercial services, owing to their flexibility and operational efficiency [1][2]. The stability and performance of UAVs are critical factors that determine their effectiveness, particularly for missions requiring precise navigation and control [3]. Recent advances in UAV technology have been driven by advances in sensor systems, artificial intelligence, and automation [4]. As these technologies continue to evolve [5], the demand for reliable stability testing methods is increasing [6][7]. To ensure UAV stability, rigorous testing in controlled environments is essential prior to deployment [8]. Traditional outdoor flight tests are often subject to unpredictable variables such as wind disturbances and GPS inaccuracies [9]. consequently, laboratory-based testing platforms, such as 3-axis gimbal rigs, offer a controlled environment for evaluating UAV performance under various simulated conditions [10].

Gimbal stabilization systems typically employ rotary encoders to track motion, providing real-time feedback for accurate positioning [12]. In this study, the LPD3806-600BM-G5 rotary encoder, known for its high-resolution angular displacement measurements, was utilized, enabling precise motion analysis [13]. The integration of this rotary encoder facilitates accurate tracking of UAV motion across multiple axes [14]. This paper outlines the design and implementation of a 3-axis UAV gimbal rig that facilitates a comprehensive examination of stability and performance parameters [15]. The gimbal system features a lightweight aluminum frame, precision bearings, and a motorized rotation mechanism, replicating real-world flight conditions [16]. Using an Arduino Nano microcontroller, the system processes encoder data and visualizes rotation metrics on a 16x2 LCD display with an I2C interface for efficient monitoring [17]. The data gathered allows for precise calibration, pre-flight adjustments, and firmware optimization [18].

A key advantage of laboratory-based testing is its ability to isolate and analyze specific motion dynamics without external interference. UAVs are subject to complex aerodynamic forces, and even minor variations in mechanical properties can significantly affect flight behavior [19][20]. This research contributes to the UAV testing methodology by providing a

laboratory-based evaluation system that ensures UAV stability before the operational deployment of machine learning algorithms and incorporates an autonomous calibration system to further enhance testing efficiency and accuracy [25].

Although several 3-axis gimbal systems have been discussed in previous studies, most focus on stabilization during flight rather than laboratory-based test rigs for UAV diagnostics. Moreover, the use of high-resolution rotary encoders (600 PPR) along with independent microcontroller control (one Arduino Nano per axis) and dedicated real-time LCD displays for each axis represents a novel, modular approach. This configuration enables parallel data processing, simplifies maintenance, and improves scalability. Thus, this research presents a unique design that addresses the gap in precise, modular, and real-time-capable test rigs for UAVs in laboratory environments.

II. METHODOLOGY

This research was carried out through several key stages, namely the design of the 3-axis gimbal system, integration of the rotary encoder, software development, and system testing in the laboratory.

A. System Design and Architecture

Define The proposed UAV 3-axis gimbal rig is designed to provide a controlled environment for testing the stability of drones

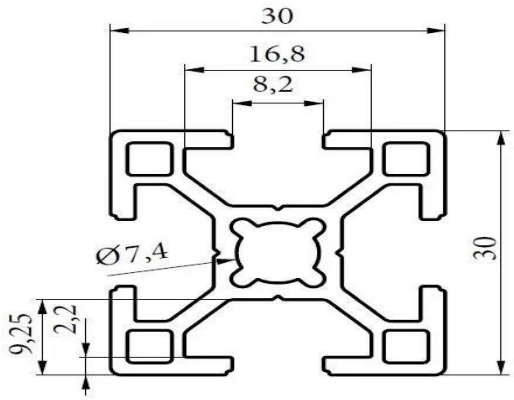

Figure 1. Alumunium Size Specification

1. Mechanical Frame: The system consists of three main components The main material used is a 30x30 mm aluminum profile, made from the aluminum alloy Al6060-T5 (a medium-strength alloy that can be heat-treated).

This material provides excellent corrosion resistance. The profile weighs 0.80 kg/m, ensuring an optimal strength-to-weight ratio, making it ideal for lightweight yet strong structural applications.

2. Rotary Encoder System: This system uses three LPD3806-600BM-G5 rotary encoders for accurate measurement of angular displacement and rotational speed. In this setup, I am using a protractor as the reference for the degree measurements.

The protractor is placed on the rotational axis to ensure the accuracy and validation of the angular measurements produced by the rotary encoders.The calibration process is carried out by matching the encoder readings with the angular scale indicated by the protractor manually. The goal is to ensure that every angular change detected by the system

Figure 2. Rotary Encoder LPD3806-600BM-G5-24C

3. This encoder has the following specifications.

- Type: AB two-phase incremental optical rotary encoder (600 pulses per revolution)
- Output Type: NPN open collector output
- Standard Cable Length: 1.5 m
- Performance: 600 pulses
- Operating Voltage: DC 5-24V
- Maximum Mechanical Speed: 5000 rev/min
- Electrical Response Frequency: 20K/sec

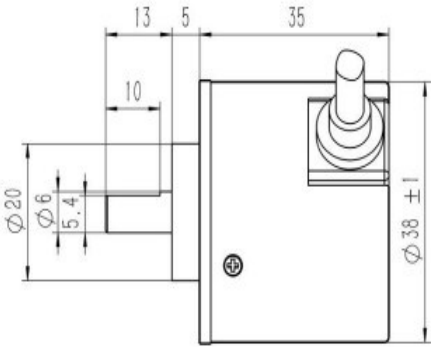

Figure 3. Rotary Encoder LPD3806-600BM-G5-24C

4. Specifications

- Encoder Body Diameter: 38 mm ± 1 mm
- Encoder Body Length: 35 mm
- Shaft Diameter: 6 mm
- Shaft Length: 13 mm
- Shaft Platform Diameter: 20 mm
- Shaft Platform Height: 5 mm
- Distance from Body to Shaft Platform: 10 mm

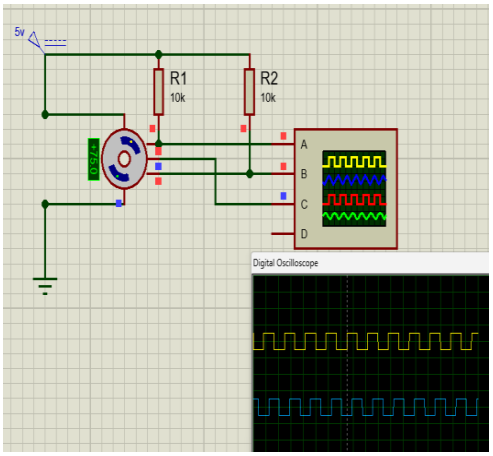

Figure 4. Characteristics of Rotary Encoder Output Data

- Quadrature Pulse Output with Two Rectangular Phases (AB) Quadrature Pulse Output with Two Rectangular Phases (AB): The encoder outputs pulses in quadrature format, with two rectangular phases (A and B), providing precise position feedback.
- Open-Collector NPN Output Type: The encoder uses an open-collector NPN output type, which can be directly connected to a microcontroller for data acquisition.
- Note: When connecting directly to an oscilloscope, a pull-up resistor must be added to ensure a proper voltage output. Without this resistor, the signal will not be observable on the oscilloscope. Ensure that the pull-up resistor is properly connected to observe the signal accurately.

5. *Microcontroller and Data Processing Unit:* The system employs three Arduino Nano microcontrollers, each linked to a 16x2 LCD via I2C. Each microcontroller is responsible for processing and displaying real-time data from a specific gimbal axis: Yaw, Pitch, and Roll.

Figure 5. 3-Axis Gimbal Display Control

- data from the rotary encoder on the yaw axis and displaying the results (such as angle position and rotation speed) on the first 16x2 LCD.
- The second Arduino Nano manages data from the encoder on the Pitch axis, with the results displayed on the second 16x2 LCD
- The third Arduino Nano controls the roll axis (longitudinal) and processes readings from the encoder as well as the current and voltage sensors. This data is displayed on the third 16x2 LCD

B. Gimbal Structure and Rotation Mechanism

The gimbal consists of three rotational axes (roll, pitch, and yaw) that enable the UAV to move freely. Each axis is driven by a motorized mechanism to ensure smooth transitions. Precision bearings installed on each axis reduce friction and enhance accuracy.

The The gimbal system is designed to simulate the UAV's dynamic motion across three axes:

1. *Z-Axis (Yaw): Left-right movement.*
2. *Y-Axis (Pitch): Up-down movement.*
3. *X-Axis (Roll): Tilting motion to the left or right (rolling).*

Each axis of the gimbal is equipped with a rotary encoder to detect rotational angles and position with high precision. The gimbal frame is constructed using lightweight yet durable aluminum to maintain structural stability and minimize vibrations that could affect measurement accuracy.

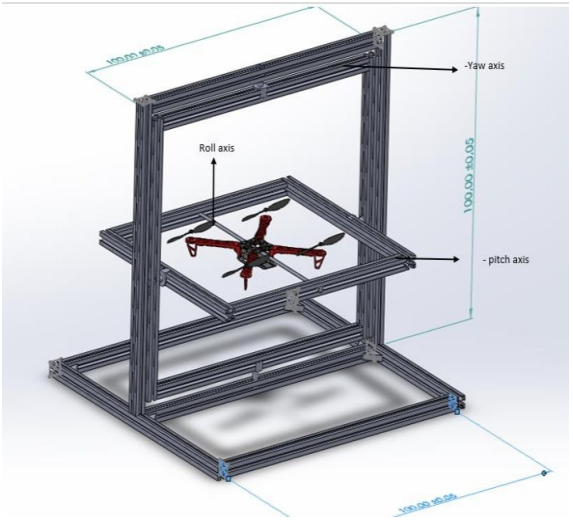

Figure.6. Mechanical Gimbal Design.

The The gimbal used for testing has a total weight of 12 kg, specifically designed to provide stability during testing. Given that its weight significantly exceeds the lifting capacity of the DJI F450 drone, which is only 2 kg, this gimbal ensures safe and optimal conditions for comprehensive drone testing.

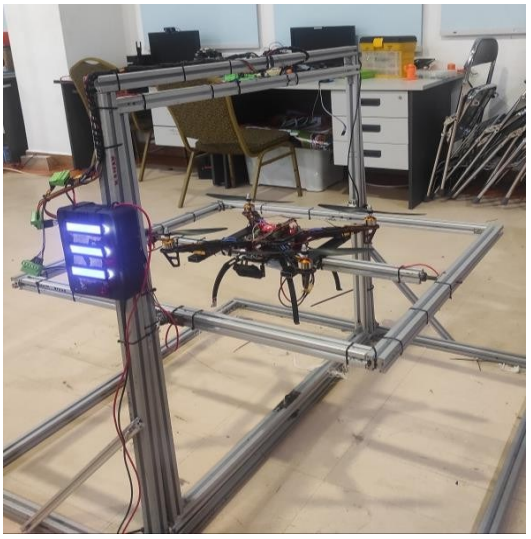

Figure.7. Base Gimbal.

The proposed three-axis UAV gimbal system consists of three primary rotational axes and two base platforms: the upper base and the lower base. The dimensions of these components are as follows:

1. *Upper Base: 100 cm x 100 cm*
2. *Lower Base: 100 cm x 100 cm*

Each rotational axis of the gimbal is designed to facilitate

dynamic movement with high precision. The dimensions for each rotational axis are as follows:

- *Axis Vertikal (Yaw): 85 cm*
- *Axis Lateral (Pitch): 75 cm*
- *Axis Longitudinal (Roll): 65 cm*

C. Sensor Integration and Data Acquisition

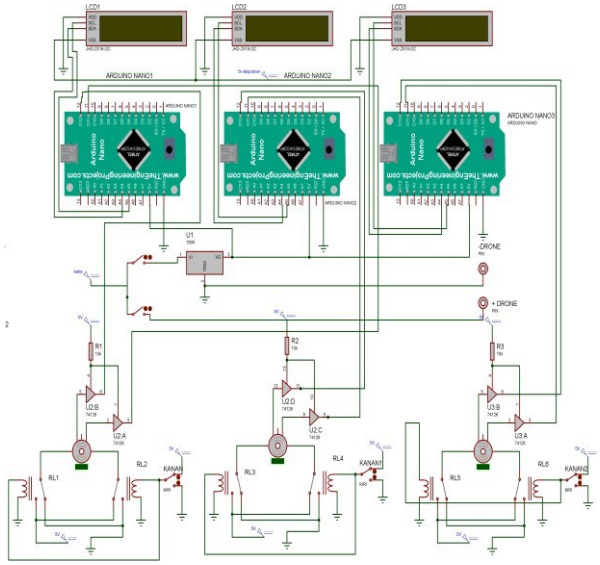

Figure.7. Wiring Diagram.

1. Integrasi Sensor Rotary Encode: A rotary encoder is utilized to measure the angular position and rotation direction of a shaft. In this system, a rotary encoder with a resolution of 600 pulses per revolution (PPR) is employed.

The quadrature-type encoder used in this study generates two pulse signals from channels A and B for each step of rotation. With a resolution of 600 steps per full revolution (360°), each step produces one pulse from each channel.

For pulse processing, Mode 1x Decoding (Rising Edge Only) is implemented, where the system counts pulses only on the rising edge of one channel (A or B). This method maintains a resolution of 600 counts per revolution (CPR) without doubling the count, as seen in Mode 2x Decoding.

By processing these pulses, the system determines both the direction and precise angular position of the rotating shaft with an accuracy level corresponding to the encoder's resolution.

2. Calculation of Angular Resolution: A rotary encoder with a resolution of 600 PPR (Pulses Per Revolution) generates pulses by detecting only the rising edge of signal the total number of pulses per full rotation (360°) remains 600 pulses.

The angular resolution, which represents the rotation per pulse, is calculated using the following formula:

- Total Pulses Per Revolution (PPR): Equation (1) In In this mode, the Arduino detects only the rising edge of signal A. As a result, the total number of pulses per full rotation (360°) is calculated as follows

$$PPR\ Total = 600 \tag{1}$$

- Equation (2) The angular resolution represents the smallest detectable change in angular position per encoder pulse. It is a critical parameter that defines the precision of angular measurements in rotary systems. Given that the encoder generates a fixed number of pulses per full revolution (360°), the angular resolution 0 res can be computed using the following expression

$$Angular\ Resolution\ = \frac{360°}{PPRtotal} = 0.6° \tag{2}$$

This implies that each pulse corresponds to an angular displacement of 0.6°, thus enabling the system to detect positional changes with this level of precision.

D. Software Implementation

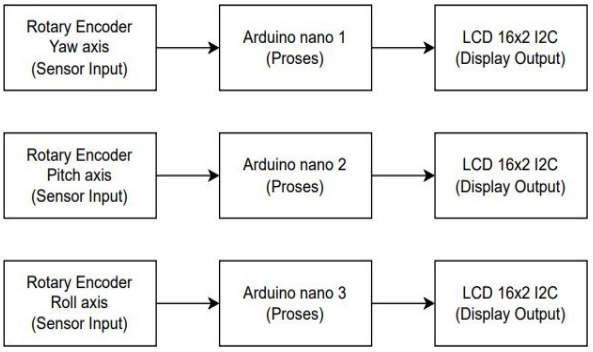

Figure.9. System Block Diagram

The software was developed using the Arduino IDE, where a custom script was written to

1. Reading Rotary EncoderValues A rotary encoder is a sensor used to detect rotational motion and generate digital pulse signals (A & B). These pulses are counted to determine the angular displacement and rotation direction (clockwise or counterclockwise).

- Rotary Encoder Yaw axis → Arduino 1
- Rotary Encoder Pitch axis → Arduino 2
- Rotary Encoder Roll axis → Arduino 3

2. Arduino Microcontroller (Data Processing) Each Arduino is responsible for reading data from a single rotary encoder and performing the following processing tasks

- Pulse Reading: The microcontroller detects and counts the pulses generated by the rotary encoder using interrupts, ensuring high accuracy and responsiveness.
- Angular Displacement Calculation: The counted pulses are converted into angular displacement (degrees) using a predefined mathematical formula.
- Rotation Direction Determination: the sequence of pulse signals, the Arduino determines whether the rotary encoder rotates in a clockwise (CW) or counterclockwise (CCW) direction.

3. Displaying Results on 16x2 I2C LCD Interface

Each Arduino is connected to an independent LCD module, displaying real-time measurements including:

- Angular displacement in degrees
- Rotation direction (CW or CCW)

III. RESULT AND DISCUSSION

A. Rotary Encoder Measurement Results

The LPD3806-600BM-G5-24C rotary encoder was calibrated using degree arc as the reference for angle measurement. During the experiment, several test scenarios were conducted to measure angular displacement and validate the accuracy of the encoder output. The results obtained are as follows:

TABLE I
CALIBRATION RESULTS FOR YAW-AXIS

Degree Arc Angle (°)	Output Encoder (Pulses)	Computed Angle (°)
1	2	1.2
5	8	4.8
15	26	15.6
30	49	29.4
60	101	60.6
90	150	90
180	301	180.6
270	452	271.2
360	598	358.8

Based on the results presented in Table I, the calibration analysis of the yaw-axis demonstrates consistent and reliable performance.

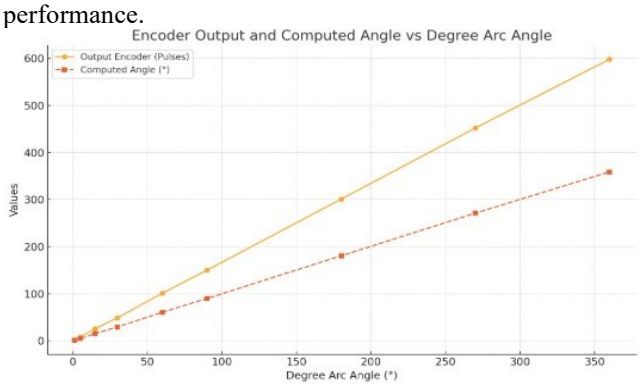

Figure.10. Yaw Axis data graph

The graph of the relationship between the rotation angle (degrees) to the encoder pulse and the calculated yaw axis angle. produces conclusions

1. *Encoder Precision:*
   - The table shows the difference between the target angle and the computed angle.
   - The computed angles closely match the target values, but small deviations still occur, especially at high angles such as 270° and 360°.
2. *Deviation Tolerance:*
   - For small angles (e.g., 1°, 5°, and 15°), the computed values match the target values, indicating high precision at low angles.
   - At larger angles, such as 360°, slight deviations are observed, showing an increase in error as the
3. *System Accuracy:*
   - The highest deviation occurs at 360°, where the computed angle is 358.8° instead of 360°.
   - Minor The lowest deviations are observed at angles below 90°, maintaining a consistent level of accuracy.
4. *The encoder provides:*
   - a pulse count proportional to the angle (e.g., 1° → 2 pulses, 360° → 598 pulses), indicating good linearity in the system

TABLE II
CALIBRATION RESULTS FOR PITCH-AXIS

Degree Arc Angle (°)	Output Encoder (Pulses)	Computed Angle (°)
1	2	1.2
5	9	45.4
15	24	14.4
30	49	29.4
60	99	59.4
90	149	89.4
180	301	180.6
270	452	271.2
360	598	358.8

Based on the results presented in Table II, the calibration analysis of the pitch-axis indicates accurate alignment and consistent system behavior, reflecting the reliability of the measurement system

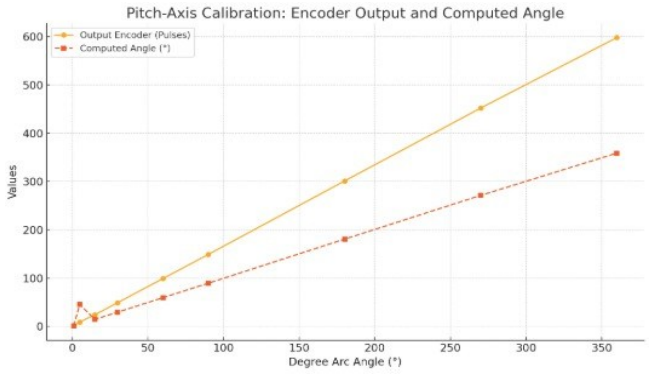

Figure.11. Pitch Axis data graph

Shows a graph of the relationship between the input angle with the encoder output pulse and the angle of the computational result. It can be seen that there is a linear relationship between the input angle and the number of output pulses, which indicates that the encoder system works consistently in detecting changes in angle. However, there is a significant anomaly at an angle of 5°, where the computational result angle is recorded at 45.4°. This indicates the possibility of an error in data collection or the computational process at that point, produces conclusions.

5. *Encoder Precision:*
   - Encoder shows a consistent linear relationship between the input angle (°) and the number of output pulses.
   - The computed angle values (red dashed line) generally follow the target angle values closely, with minor deviations observed at certain points.
6. *Deviation Tolerance:*
   - For small angles such as 1° and 15°, the computed values are highly accurate and closely match the target values.
   - However, a significant anomaly occurs at 5°, where the computed angle spikes unusually. This suggests a possible data reading error or computational error at that point.

7. *System Accuracy:*
   - The system demonstrates the highest accuracy at angles below 60°, excluding the outlier at 5°, where the computed angles are very close to the actual input.

TABLE III
CALIBRATION RESULTS FOR ROLL AXIS

Degree Arc Angle (°)	Output Encoder (Pulses)	Computed Angle (°)
1	2	1.2
5	8	4.8
15	26	15.6
30	49	29.4
60	101	60.6
90	149	89.4
180	301	180.6
270	452	271.2
360	598	358.8

As presented in Table III, the roll-axis calibration analysis demonstrates.

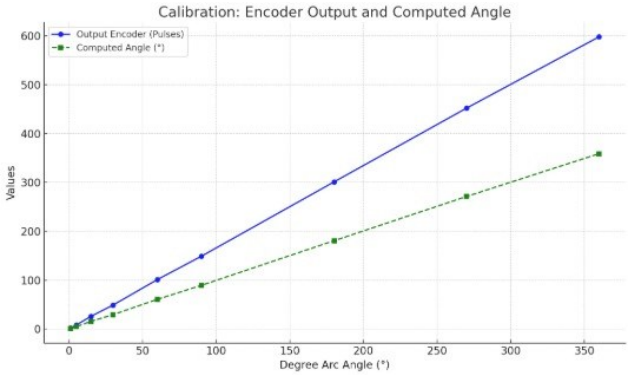

Figure.12. Roll Axis data graph

Shows a graph of the relationship between the input angle and two important parameters, namely the encoder pulse and the computational angle. Calibration testing is carried out to verify the consistency and accuracy of the encoder readings against changes in the roller axis angle. The calibration results are presented in Table , which shows the relationship between the input angle, the number of pulses generated by the encoder and the computational angle. From the graph, the following conclusions can be drawn

8. *Encoder Precision:*
   - The computed angles closely match the target angles with minor deviations across the range.
   - At higher angles, such as 270° (computed: 271.2°) and 360° (computed: 358.8°), small deviations are observed but remain within acceptable tolerances.
9. *Deviation Tolerancengles (30°, 60°, and 90°):*
   - At smaller angles (e.g., 1°, 5°, and 15°), the computed angles closely align with the target angles, showing high precision at low angles.
   - Slight deviations appear at higher angles, such as 360° (computed: 358.8°), demonstrating a minor increase in error at these ranges.

B. Comparison Between Axes

This document presents a comprehensive comparison of the calibration results for the yaw, pitch, and roll axes. The analysis is based on the data provided in the respective tables, which include detailed measurements for each axis. Specifically, the comparison focuses on the Output Encoder values measured in pulses and the corresponding Computed Angle in degrees (°).

TABLE IV
COMPARISON OF OUTPUT ENCODER (PULSES)

Degree Arc Angle (°)	Yaw Axis	Pitch Axis	Roll Axis
1	2	2	2
5	8	9	8
15	26	24	26
30	49	49	49
60	101	99	101
90	150	149	149
180	301	301	301
270	451	452	452
360	598	598	598

As shown in Table IV, the calibration data for the yaw, pitch, and roll axes demonstrate consistent encoder output values across varying arc angles, confirming the reliability of the system's angular response.

TABLE V
COMPARISON OF COMPUTED ANGLES (°)

Degree Arc Angle (°)	Yaw Axis	Pitch Axis	Roll Axis
1	1.2	1.2	1.2
5	5.4	5.4	4.8
15	14.4	14.4	15.6
30	29.4	29.4	29.4
60	60.6	59.4	60.6
90	90	89.4	89.3
180	180.6	180.6	180.6
270	271.2	271.2	271.2
360	358.8	358.8	358.8

Table V shows that the computed angles for the yaw, pitch, and roll axes closely match the corresponding input degree arc angles, indicating that the calibration process yields precise and reliable angular measurements.

C. Analysis and Observations

1. The Output Encoder (Pulses) values: are relatively close across all three axes, with minor variations at some points.
2. The Computed Angle (°) values: follow a similar trend, but slight differences are observed at 1°, 5°, 60°, 270°, and 360°.
3. The pitch axis: tends to have slightly higher computed angles at lower values, whereas the roll axis has slightly lower values at 360°.
4. Overall: the calibration appears consistent, but slight variations may be due to encoder precision, calibration methodology, or data rounding.

D. Discussion of Results

1. Comparison with Previous Rigs, The design proposed in this study offers a cost-effective open-source solution with a focus on measuring the angle of motion of the UAV axis. The system uses three independent Arduino Nano units, each connected to a single 16x2 LCD, which allows data processing and display to be carried out in parallel and in real-time.

This is a striking difference from conventional designs that typically use centralized control and a single main display screen.The design also uses a high-resolution rotary encoder (600 PPR) for each axis, resulting in angular accuracy with maximum deviation ±1.2° at full rotation. This makes the system more precise compared to some previous designs that only used low-resolution encoder.

2. Key Advantages of the Proposed Design These 3-axis Gimbal rigs show significant advantages in terms of cost, ease of replication, accuracy, and testing flexibility. The lightweight aluminum frame is designed to remain robust and have minimal vibration during UAV testing, providing stability during rotational angle data capture.

This design utilizes three independently working Arduino Nano units, each handling a single axis with a single 16x2 LCD screen, allowing data readings and displays to be done in real-time without interruption between axes. In addition, the angle data display can be changed via the push-button on each unit, providing convenience in monitoring each axis separately. This modular approach not only simplifies system maintenance, but also opens up opportunities for the development of additional features in the future, which are generally difficult to implement in commercial-based closed systems.

3. System Limitations, Direct testing with UAVs could not be performed during this stage of the project as the UAV unit of the responsible division was not yet available at the time this research was completed. Nevertheless, the gimbal rig system was thoroughly tested through manual axis rotation and angle validation using a protractor. These tests demonstrated that the system operates with high accuracy and stability, indicating its readiness for future integration into real UAV testing scenarios.

Although the designed 3-axis gimbal rig demonstrated good angular measurement accuracy under controlled testing conditions, several limitations should be noted.

While the Arduino Nano used in this system still provides sufficient I/O pins to support the addition of some extra sensors or modules, future system expansion must consider its limited processing capability and memory, especially if advanced features such as automatic data logging, wireless communication, or complex sensor integration are to be implemented

The most significant mechanical limitation lies in the inability of the gimbal to perform continuous rotation on each axis. This is due to the wiring layout, where cables pass between each base axis of the gimbal. During testing, the system was capable of safely completing a full 360-degree rotation; however, exceeding this range risks cable tension and potential damage. As a result, the rig is only suitable for limited-range laboratory testing rather than unrestricted continuous rotation.

IV. CONCLUSION

In this chapter, an analysis of the calibration for each axis of the angle and pulse encoding system is presented. Based on the measurement and calculation results, several important conclusions regarding the accuracy and performance of the system can be drawn.

Based on the calibration results, it can be concluded that the pulse output encoding system provides highly accurate results in converting pulse encodings to degree angles. The detected tolerances for most calibration points are very small, with tolerance values remaining below 1% for the majority of measurements. This indicates that the system has excellent accuracy.

Based on the analysis conducted, the pulse encoding system used has proven to be reliable for angle measurement applications. Although there is some minor deviation, this can be considered acceptable in the context of technical applications where high precision is required, such as in yaw axis control in mechanical or robotic systems.

Although the calibration results demonstrate good performance, there is still room for further improvement by reducing tolerances at specific points. Further research on material selection, sensor types, or even calibration methods can be conducted to enhance the system's accuracy, particularly at extreme points such as 270° and 360°.

.

REFERENCES

[1] R. Casado and G. Ferna, "Drone challenge : A platform for promoting programming and robotics skills in K-12 education," no. February, pp. 1–19, 2019, doi: 10.1177/1729881418820425.

[2] S. Samsugi, Z. Mardiyansyah, and A. Nurkholis, "Sistem Pengontrol Irigasi Otomatis Menggunakan Mikrokontroler Arduino Uno," *J. Teknol. dan Sist. Tertanam*, vol. 1, no. 1, p. 17, 2020, doi: 10.33365/jtst.v1i1.719.

[3] U. Fadlilah and N. Saniya, "Monitoring Suhu Kabel Trafo melalui Tampilan LCD dan SMS," *Emit. J. Tek. Elektro*, vol. 17, no. 2, pp. 42–49, 2017, doi: 10.23917/emitor.v17i2.6229.

[4] D. Xia, L. Cheng, and Y. Yao, "A robust inner and outer loop control method for trajectory tracking of a quadrotor," *Sensors (Switzerland)*, vol. 17, no. 9, 2017, doi: 10.3390/s17092147.

[5] S. Ahirwar, R. Swarnkar, S. Bhukya, and G. Namwade, "Application of Drone in Agriculture," *Int. J. Curr. Microbiol. Appl. Sci.*, vol. 8, no. 01, pp. 2500–2505, 2019, doi: 10.20546/ijcmas.2019.801.264.

[6] D. Giuseppe and G. Adrián, "MOUNTED ON A GYROSCOPIC TEST," pp. 1–170, 2023.

[7] W. Rahiman, "Infrared Sensor and PWM Integration Using FPGA Platform for Ground Vehicle Navigation and Speed Control," vol. 1, no. 1, pp. 1–8, 2021.

[8] A. Iannarelli, M. G. Niasar, and R. Ross, "Sensors and Actuators A : Physical Electrode interface polarization formation in dielectric elastomer actuators," *Sensors Actuators A. Phys.*, vol. 312, p. 111992, 2020, doi: 10.1016/j.sna.2020.111992.

[9] O. I. Adebisi, A. B. Ogundare, T. C. Erinosho, M. O. Sonola, and A. R. Adesanu, "Development of a microcontroller and resistive touchscreen-based speed monitoring and control system for DC motor," *Int. J. Adv. Appl. Sci.*, vol. 12, no. 4, pp. 350–360, 2023, doi: 10.11591/ijaas.v12.i4.pp350-360.

[10] S. J. Sutanto and B. W. Ridwan, "Teknologi Drone Untuk Pembuatan Peta Kontur: Studi Kasus Pada Kawasan P3Son Hambalang," *J. Tek. Hidraul.*, vol. 7, no. 2, pp. 179–194, 2016.

[11] K. Castelli and H. Giberti, "Additive manufacturing as an essential element in the teaching of robotics," *Robotics*, vol. 8, no. 3, pp. 1–13, 2019, doi: 10.3390/robotics8030073.

[12] E. N. Afifah Amatullah, R. Ekawita, and E. Yuliza, "Comparison of Infrared and Optocoupler Sensors Performance for Lab-Scale Rpm Measurement System," *Indones. Phys. Rev.*, vol. 5, no. 2, pp. 130–136,

2022, doi: 10.29303/ipr.v5i2.150.
[13] P. Sapkota, N. Pokharel, R. Silwal, S. Chitrakar, H. P. Neopane, and B. Thapa, "Rotational Speed Measurement of a Shaft Using Infrared Sensor with NI Data Acquisition system and LabVIEW," *J. Phys. Conf. Ser.*, vol. 2629, no. 1, 2023, doi: 10.1088/1742-6596/2629/1/012020.
[14] M. J. Mnati, A. Van den Bossche, and R. F. Chisab, "A smart voltage and current monitoring system for three phase inverters using an android smartphone application," *Sensors (Switzerland)*, vol. 17, no. 4, 2017, doi: 10.3390/s17040872.
[15] T. Lisec, S. Fichtner, N. Funck, M. Claus, B. Wagner, and F. Lofink, "Sensors and Actuators A : Physical AlScN based MEMS quasi-static mirror matrix with large tilting angle and high linearity," *Sensors Actuators A. Phys.*, vol. 312, p. 112107, 2020, doi: 10.1016/j.sna.2020.112107.
[16] A. Sudarmaji, A. Y. Putra, and E. Yudiarsah, "Viscous Damping Coefficient Measurement System Using Incremental Optical Encoder," *FLYWHEEL J. Tek. Mesin Untirta*, no. June 2023, p. 1, 2023, doi: 10.36055/fwl.v0i0.19525.
[17] M. Khaleel, M. Emimi, and A. Alkrash, "The Current Opportunities and Challenges in Drone Technology International Journal of Electrical Engineering and Sustainability (IJEES) The Current Opportunities and Challenges in Drone Technology," *Int. J. Electr. Eng. Sustain.*, vol. 1, no. 3, pp. 74–89, 2023, [Online]. Available: https://ijees.org/index.php/ijees/index
[18] R. A. Firmansyah, Y. A. Prabowo, T. Suheta, A. Nanda, and D. Utomo, "MITOR : Jurnal Teknik Elektro," 2024.
[19] B. Şimşek and H. Ş. Bilge, "A novel motion blur resistant vslam framework for micro/nano-uavs," *Drones*, vol. 5, no. 4, 2021, doi: 10.3390/drones5040121.
[20] W. Wójcik *et al.*, "Metrological Aspects of Controlling the Rotational Movement Parameters of the Auger for Dewatering Solid Waste in a Garbage Truck," *Int. J. Electron. Telecommun.*, vol. 69, no. 2, pp. 233–238, 2023, doi: 10.24425/ijet.2023.144355.
[21] J. Paik, M. Carlson, Z. Richter, T. Van, D. Berg, and R. Zhan, "Automated Drone Calibration System Final Design Review Inspired Flight Calibration Team," no. June, 2020.
[22] V. Oguntosin and A. Akindele, "Design of a joint angle measurement system for the rotary joint of a robotic arm using an Incremental Rotary Encoder," *J. Phys. Conf. Ser.*, vol. 1299, no. 1, 2019, doi: 10.1088/1742-6596/1299/1/012108.
[23] Z. S. Islami and F. Hartono, "Development of small propeller test bench system," *IOP Conf. Ser. Mater. Sci. Eng.*, vol. 645, no. 1, 2019, doi: 10.1088/1757-899X/645/1/012017.
[24] U. Veyna, S. Garcia-Nieto, R. Simarro, and J. V. Salcedo, "Quadcopters testing platform for educational environments," *Sensors*, vol. 21, no. 12, 2021, doi: 10.3390/s21124134.
[25] Azhari, T. I. Nasution, S. H. Sinaga, and Sudiati, "Design of Monitoring System Temperature And Humidity Using DHT22 Sensor and NRF24L01 Based on Arduino," *J. Phys. Conf. Ser.*, vol. 2421, no. 1, 2023, doi: 10.1088/1742-6596/2421/1/012018.